

RESEARCH

Concentrations, Loads, and Associated Trends of Nutrients Entering the Sacramento–San Joaquin Delta, California

Dina Saleh*¹, Joseph Domagalski¹

ABSTRACT

Statistical modeling of water-quality data collected at the Sacramento River at Freeport and San Joaquin River near Vernalis, California, USA, was used to examine trends in concentrations and loads of various forms of dissolved and particulate nitrogen and phosphorus that entered the Sacramento–San Joaquin River Delta (Delta) from upstream sources between 1970 and 2019. Ammonium concentrations and loads decreased at the Sacramento River site from the mid-1970s through 1990 because of the consolidation of wastewater treatment and continuously reduced from the mid-1970s to 2019 at the San Joaquin River site. Current ammonium concentrations are mostly below $4\ \mu\text{M}$ ($0.056\ \text{mg N L}^{-1}$) at both sites, a concentration above which reductions in phytoplankton productivity or changes in algal species composition may occur. The Sacramento River at Freeport site is located upstream of the Sacramento Regional County Sanitation District's treatment facility's discharge point;

nutrient water quality there is representative of upstream sources. Inorganic nitrogen (nitrate plus ammonium) concentrations and loading differed at both sites. At the Sacramento River location, concentrations decrease in the summer agricultural season, reducing the molar ratios of nitrogen to phosphorus.

In contrast, inorganic nitrogen concentrations increase in the San Joaquin River during the agricultural season as a result of irrigation runoff, increasing the molar ratio of nitrogen to phosphorus. This increase suggests a possible nitrogen limitation in the northern Delta and a phosphorus limitation in the southern Delta, as indicated by the molar ratios of bioavailable nitrogen to bioavailable phosphorus. Planned upgrades to the Sacramento Regional Wastewater Treatment Plant (SRWTP) will reduce inorganic nitrogen inputs to the northern Delta. Consequently, the supply of bioavailable nitrogen throughout the upper estuary should diminish. Source modeling of nitrogen and phosphorus identifies agriculture, atmospheric deposition, and wastewater effluent as sources of total nitrogen in the Central Valley. In contrast, geologic sources, agriculture, and wastewater discharge are the primary sources of phosphorus.

SFEWS Volume 19 | Issue 4 | Article 6

<https://doi.org/10.15447/sfew.2021v19iss4art6>

* Corresponding author: dsaleh@usgs.gov

¹ California Water Science Center
US Geological Survey
Sacramento, CA 95819 USA

KEY WORDS

Sacramento–San Joaquin Delta, nutrient loads, nutrient trends, WRTDS model, SPARROW model, water quality, total nitrogen, total phosphorous

INTRODUCTION

The Sacramento–San Joaquin River Delta (Delta) is part of the largest estuary on the west coast of North America, covering an area of about 2,984 km². The Delta is an essential source of water for both urban and agricultural users by way of pumps in the southern portion (Templin and Cherry 1997; <https://water.ca.gov/Programs/State-Water-Project/Management/Water-Transfers>). About 2,024 km² of the Delta is agricultural land and home to many bird, mammal, and fish species. The Delta receives most of its freshwater from the combined flows of the Sacramento and San Joaquin rivers, which collectively drain about 100,000 km² of land with a diverse land cover. Spatial distribution of different land cover in the study area, as classified in the U.S. Geological Service (USGS) National Land Cover Database (NLCD) 2001 digital data (https://www.usgs.gov/centers/eros/science/national-land-cover-database?qt-science_center_objects=0#qt-science_center_objects), is shown in Figure 1. The Sacramento and San Joaquin rivers deliver freshwater to the Delta, with annual inputs of about 84% from the Sacramento River, 13% from the San Joaquin River, and 3% from other smaller rivers (Jassby and Cloern 2000; Saleh and Domagalski 2015). Water management for flow and water quality requires that numerous decisions need to be made, many of them daily, regarding reservoir releases, diversions, aquatic species management, and environmental flows to protect water quality (Luoma et al. 2015; Norgaard et al. 2009). The hydrology of the Delta under natural conditions has been described by Fox et al. (2015).

In recent years, it has been suggested that the forms of nutrients and nutrient stoichiometry, especially the relative amounts of ammonium versus nitrate but also nitrogen versus phosphorus, may cause changes in primary productivity—particularly the abundance and species composition of phytoplankton that affect

open-water food webs in the Delta (Glibert 2010; Parker et al. 2012). The potential effects on the ecosystem from ammonium in wastewater discharge prompted the California Central Valley Water Quality Control Board (CVWQCB) to issue new discharge requirements for one of the most significant dischargers of wastewater to the Delta: the Sacramento Regional County Sanitation District's (Regional San's) treatment facility (<https://www.regionalsan.com/echowater-project>). Mandated upgrades to the Regional San facility include biological nutrient removal that will remove most of the ammonium via nitrification, and a portion of the nitrate via denitrification (Krich–Brinton 2017). In addition, the upgrades may result in some phosphorus removal (West Yost Associates 2011), although these are expected to be minor. These upgrades will decrease the nutrient load from the treated wastewater effluent and may result in ecosystem changes (<https://www.regionalsan.com/echowater-project>, https://www.usgs.gov/centers/ca-water/science/evaluating-effects-wastewater-derived-nutrients-phytoplankton-abundance-and-qt-science_center_objects=0#qt-science_center_objects). Other treatment plants that discharge to the Delta are also upgrading their facilities or management of their effluents. These include the Modesto Water Quality Control facility, the Turlock Regional Water Quality Control facility, and the Stockton Regional Wastewater Control facility (see Figure 1). Anthropogenic changes in nutrient stoichiometry can also be caused by other processes, including agriculture and the presence of dams or other impoundments (Maavara et al. 2020).

Once these upgrades are operational, a change will be expected in the amount of inorganic nitrogen that enters the Delta, especially the North Delta. Ongoing research addresses how these changes may affect the Delta ecosystem (Richey et al. 2018). To better understand the future effects of these planned changes on nutrient availability and transport to the Delta, we used two water quality models coupled with long-term monitoring to evaluate historical nutrient loads and trends in the Sacramento and San Joaquin rivers, and to assess the major sources of nutrients in these two watersheds.

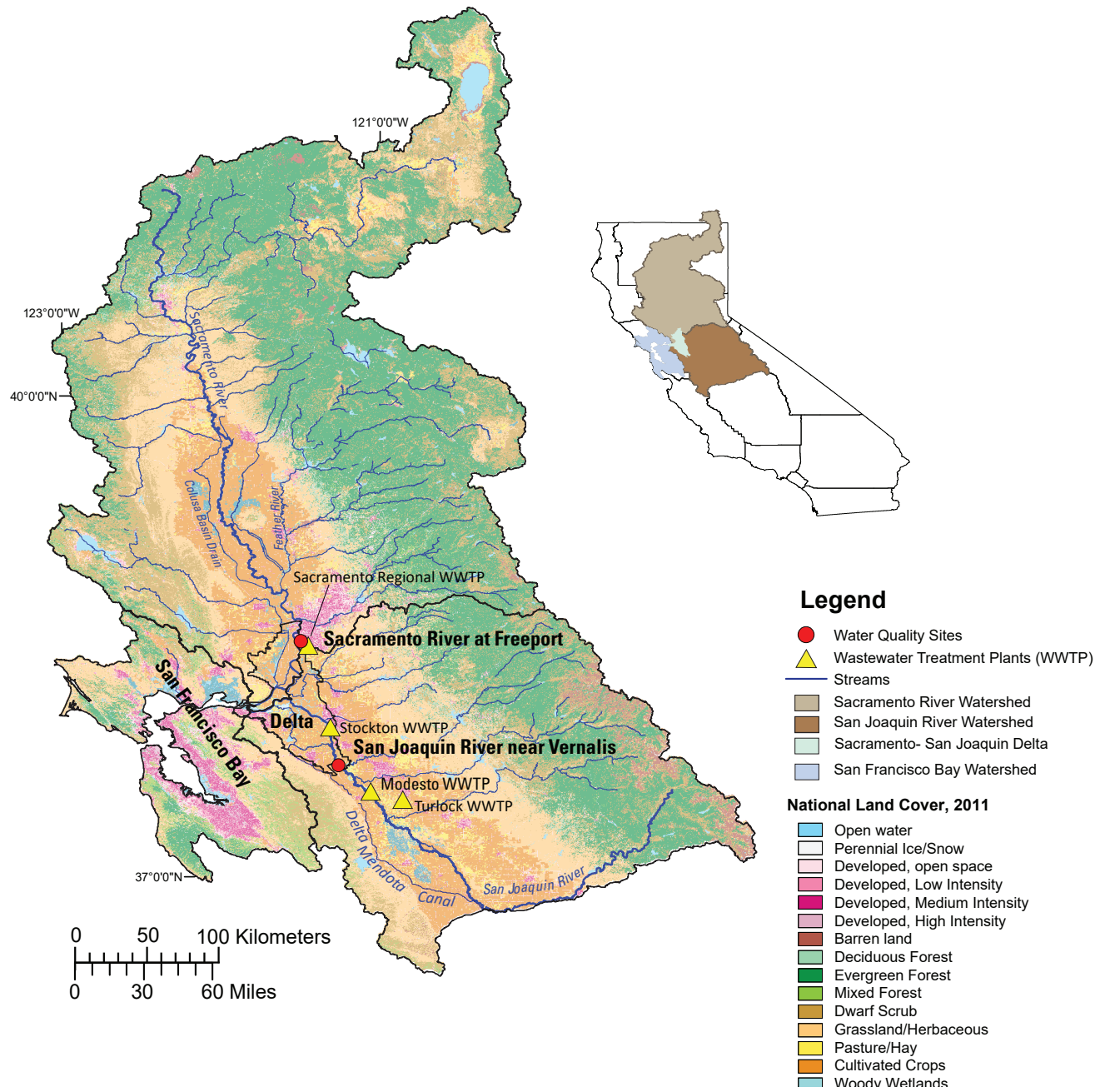


Figure 1 Location of the two water quality sampling sites, geographic extent of the Sacramento and San Joaquin River watersheds, and San Francisco Bay watershed, Sacramento–San Joaquin Delta, and locations of selected wastewater treatment plants. Land cover as classified in the USGS National Land Cover Database (NLCD) 2001 digital data. (Source: https://www.usgs.gov/centers/eros/science/national-land-cover-database?qt-science_center_objects=0#qt-science).

The upstream sources provide large loads of nitrogen and phosphorus in various forms, which affect the forms of nutrients—such as relative amounts of nitrate, ammonium, and organic nitrogen—and the respective ratios of nutrients—especially bioavailable forms such as nitrate and orthophosphate—that enter the North and South Delta. Understanding nutrient concentrations, loads, and sources may be helpful in future decisions about ecosystem management of the Delta. A multi-year record of monitoring data (1970 through 2019) is available for the various forms of nitrogen and phosphorus at two locations: the Sacramento River at Freeport and the San Joaquin River near Vernalis (Figure 1). These two rivers provide most of the freshwater to the Delta, and drain large watersheds with complex land uses, including agriculture, urban, and natural areas such as forested land. We used information from these two sites and the upstream watersheds to evaluate historical nutrient concentrations, loads, and sources; the upstream spatial distribution of nutrient sources throughout the watersheds; and nutrient transport to the Delta along the river courses. The record of discrete sampling captures various weather conditions, including wet years (1997, 2017) and drought years (2012 through 2016). Trend estimation for nitrate, ammonium, Kjeldahl nitrogen (organic N plus ammonium), total nitrogen (TN), orthophosphate (OP), and total phosphorus (TP) concentrations and loads, allows managers to understand the watersheds' contribution of various forms of nutrients as they enter the Delta and support aquatic food webs. For trend analysis, we used the weighted regressions on time, discharge, and seasons (WRTDS) method (Hirsch et al. 2010). This model provides statistical characterizations of the concentrations and loads, as well as graphical capabilities to display the trends. The WRTDS model utilizes discrete data collected over at least 20 years to produce the trend models.

The WRTDS model output also allows nutrient ratios to be examined. Molar ratios of key nutrients such as bioavailable nitrogen and phosphorus, or nitrate and ammonium, are important to understand how the

aquatic ecosystem might respond to varying concentrations of key nutrients on an annual cycle. A molar ratio of carbon-to-nitrogen-to-phosphorus for marine systems has been proposed as 106:16:1 (Redfield 1958). This ratio was based on molar concentrations in marine algae. Bioavailable nutrient concentrations in water were thought to reflect these ratios, and if the N:P ratio drops below 16, nitrogen is considered a limiting nutrient; above 16, phosphorus is considered the limited nutrient. For freshwater aquatic systems, a ratio of N:P of 24:1 has been proposed (Maranger et al. 2018). Recent studies have shown that anthropogenic activities can affect these ratios. For example, Maavara et al. (2020) showed that reservoirs can alter these ratios by accumulating phosphorus in sediments. And Domagalski et al. (2021) showed that forest growth and fire suppression can alter ratios. The concentration trends at two locations were paired with upstream modeling, using the SPATIally Referenced Regressions On Watershed attributes (SPARROW) model (Preston et al. 2009), to determine the sources of TN and TP throughout the Sacramento and San Joaquin river valleys. The SPARROW model requires a suitable number of calibration sites throughout a watershed, as well as knowledge of potential sources, including atmospheric, agricultural, land use, geological background, and landscape factors that affect transport, which include soil characteristics, river courses, river depths, etc. These two approaches provide information on nutrient trends and loads at two essential inputs to the Delta, as well as the most probable upstream sources. This analysis focuses on nutrient concentrations and loads at the two major river locations where most of the water enters the Delta. It was beyond the scope of this paper to consider changes or trends in nutrient concentrations downstream of those two locations. Our analysis focuses on the upstream sources of nutrient concentrations and load trends where the Sacramento and San Joaquin rivers enter the Delta. Previous work on this part of the Delta has been reported on by Schlegel and Domagalski (2015). Schlegel and Domagalski (2015) also discussed trends, up to 2013, for TN, ammonium, nitrate, and TP for the two sites of this study, and for upstream sites

in both the Sacramento and San Joaquin rivers. Nutrient trends within the estuary and the inflow streams to the Delta have also been reported on by Beck et al. (2018), who discussed trends in nitrate, ammonium, and silica at the two sites of this study and within the estuary up to 2013. This study expands on the previous investigations of the sites by extending the study period to 2019, by including the previously modeled nutrients and bioavailable orthophosphate, and by examining upstream watershed sources of TN and TP.

STUDY AREA AND DATA SOURCES

The Sacramento and San Joaquin rivers are the two largest rivers in California, delivering annually, on average, about $650 \text{ m}^3 \text{ s}^{-1}$ and $120 \text{ m}^3 \text{ s}^{-1}$ of water, respectively, to the Delta. Both river systems contain many upstream diversions and impoundments designed to provide flood protection, ensuring reliable drinking water and irrigation water to over 2 million Californians (Kratzer et al. 2011). Nutrients enter the Delta primarily through the Sacramento and San Joaquin rivers from sources including agricultural activities, atmospheric deposition, municipal wastewater treatment plant (WWTP) inputs, scrub and grassland, urban areas, and underlying geology.

We obtained concentration data for nitrate, ammonium, total Kjeldahl nitrogen, OP, TP, and TN (TN is the sum of nitrate and Kjeldahl nitrogen) for the study from various sampling programs at the two USGS stream gauge locations: Sacramento River at Freeport (USGS site identification code 11447650) and the San Joaquin River near Vernalis (USGS site identification code 11303500) over the 1970-through-2019 period. Not all nutrients had the same period of record, and the full record for each nutrient was always used to calculate the trends. We made no substantive changes to analytical methods used for nutrient measurements that would affect the data analysis for this period of record. All nutrient data were well above the method recording limits, and no censored data were present. We obtained all the discharge data and most water quality data from the USGS National Water Information System

(NWIS, <https://doi.org/10.5066/F7P55KJN>; USGS 2020); other additional water quality data came from a previously published report (Kratzer et al. 2011). These two sites selected for this study were sampled frequently (more than 500 samples) from 1970 through 2019, and have a continuous record of streamflow data concurrent with the water-quality records at these sites.

METHODS

Turnipseed and Sauer (2010) and Sauer and Turnipseed (2010) described river discharge measurement methods used by the USGS. Other methodology—for example, acoustic Doppler current profiling—is necessary at tidally influenced stations, such as the Sacramento River at Freeport. The methods used on the Sacramento River site are summarized by Burau et al. (2015).

Nutrients were analyzed at the USGS laboratory as described by Fishman et al. (1993). Because different sampling programs collected and analyzed nutrients at these two sites, the period of record was not the same at the two locations. Analytical methods did not change, and all analyses were above the method detection or reporting limits, so any change in method detection or reporting did not affect the data set. Not all nutrients had the same period of record, and the full record for each nutrient was always used to calculate the trends. The Sacramento River at Freeport site had over 500 nutrient analyses, and the San Joaquin River near Vernalis site had over 800 analyses. We used the most extended period of record to calculate the best trend information. We estimated concentrations, mass loads, and trends using the WRTDS model (Hirsch et al. 2010). We assessed watershed sources of nutrients (TN and TP) using the SPARROW model (Preston et al. 2009, 2011).

The WRTDS model is written in the R computing framework and is publicly available from the Comprehensive R Archive Network (CRAN) (<https://www.R-project.org>). The WRTDS model is part of the EGRET package and is directly available from CRAN. We used EGRET version 3.0.2 for WRTDS calculations. Confidence

intervals and statistical significance of the load and trend models were completed with EGRETci (version 2.0.3), also available from CRAN. The model was developed to produce estimates of concentration and load, along with the ability to calculate flow-normalized estimates of concentration and load with graphical capabilities to illustrate the resulting trends. WRTDS evaluates a concentration–discharge relationship based on time, discharge, and season by re-evaluating coefficients for each estimation day. The estimated concentration is a product of the following equation:

$$\ln(c) = \beta_0 + \beta_1 t + \beta_2 \ln(Q) + \beta_3 \sin(2\pi t) + \beta_4 \cos(2\pi t) + \varepsilon \quad (1)$$

Where, c is the concentration in mg L^{-1} , Q is the mean daily discharge in $\text{m}^3 \text{s}^{-1}$, t is the time in decimal years, β_{0-4} are fitted coefficients, and ε is the unexplained variation (Hirsch et al. 2010). Statistical significance of the calculated loads is given by a bias statistic. Most of those indicated a favorable model with a bias statistic of plus or minus 1% to 10%. Estimates of concentration and load are presented on a daily to annual time-scale. A flow-normalization calculation provides further information about how concentrations and loads change with time. Within an annual period, variations in streamflow measurements at any given site over the period of the record may be natural, such as a flood and drought cycles, or through water management. To deal with discharge variations, the flow-normalized-concentrations (FNC) approach is used in WRTDS (Hirsch et al. 2010). The FNC is defined as:

$$E[C_{fn}(T)] = \int_0^{\infty} w(Q, T) \cdot f_{Ts}(Q) dQ, \quad (2)$$

where $E[C_{fn}(T)]$ is the flow-normalized concentration for time T (a specific day of a particular year); $w(Q, T)$ is the WRTDS estimate of concentration as a function of Q , which is discharge and time T (time in years); and $f_{Ts}(Q)$ is the probability density of discharge specific to a particular time of year designated as T_s . T_s is restricted to values between 0 and 1, the decimal portion of the year, and is defined as the fractional part of the time variable T (Hirsch et

al. 2015). Trends in concentration or load, and their significance levels, were calculated using the EGRETci R package. The EGRETci R package uses a bootstrap method and an adaptive Bayesian approach to evaluate when to accept or reject the null hypotheses (Hirsch et al. 2015). The tests provide a two-sided p -value associated with the null hypothesis and confidence intervals and uses an alpha level (α) of 0.1 for each of the tests (Hirsch et al. 2015). Confidence intervals (90%) are calculated on the flow-normalized trend. A value of 0.1 is used, instead of a more traditional value of 0.05, to have a high probability of identifying real trends. This is a trade-off between detecting a real trend against detecting one when no trend exists (Hirsch et al. 2015). A term, denoted as π_f is the fraction of bootstrap replicates in an infinite number of bootstrap replicates, for which the estimated change in flow-normalized flux is positive. An estimate can be made at any stage of the bootstrap process denoted as $\hat{\pi}_f$. That term is defined as the mean of the Bayesian posterior distribution of π_f . A full description is given in Hirsch et al. (2015). Definitions for determining the statistical significance of a trend direction, provided by the function of $\hat{\pi}$, are shown in Table 1. Within any trend direction, a “Highly Likely” trend means there is at least a 95 out of 100 chance of a statistically significant trend in that direction; a “Very Likely” trend means there is a 90 to 95 out of 100 chance that the trend would be in a specific direction; and, finally, a “Likely” trend means there is a 66 to 90 out of 100 chance of a trend in that direction. Along with the likelihood and the direction of trend for each constituent, EGRETci output also provides an estimated change value for concentrations and loads in mg L^{-1} and kg yr^{-1} , respectively.

We completed trends in daily streamflow using a non-parametric Mann–Kendall approach using various R packages (Kendall, version 2.2; *rkt*, version 1.5; *zyp*, version 0.1-1.1; *lubridate*, version 1.7.10; *zoo*, version 1.8-9; <https://owi.usgs.gov/blog/Quantile-Kendall/>). We compiled statistics for a 7-day minimum discharge, a 7-day maximum discharge, a median daily discharge, and a mean daily discharge. We compiled statistical results across the range of non-exceedance probabilities.

Table 1 Definitions for descriptive statements of trend likelihoods for WRTDS bootstrap test as a function of $\hat{\pi}$, the posterior mean estimate of the probability of an increasing trend (Hirsch et al. 2015)

Range of $\hat{\pi}$ Values	Descriptors
≥ 0.95 and ≤ 1.0	Highly Likely
≥ 0.9 and < 0.95	Very Likely
≥ 0.66 and < 0.90	Likely
> 0.33 and < 0.66	About as Likely as Not
> 0.1 and ≤ 0.33	Unlikely
> 0.05 and ≤ 0.1	Very Unlikely
≥ 0 and ≤ 0.05	Highly Unlikely

SPARROW models used in this report are based on average climatic conditions, such as rainfall, and hydrological conditions, usually a 30-year average. Land use or other variables used to determine sources and transport of nutrients are identified from a base year, in this case, 2012. Although the SPARROW model utilizes these long-term averages and one base year, the model can identify and quantify nutrient sources within a large watershed, and hydrological and bio-geochemical alteration of the nutrients along riverine flow paths. We use the SPARROW model to identify the source areas of nutrients and amounts of nutrients that reach the locations for trend analysis. Thus, information is gained on how nutrients are sourced: atmospheric, agricultural, urban, point sources, and other landscape sources. De-trending some of the calibration data, such as streamflow, takes out the year-to-year variations and allows nutrient sourcing and transport under average conditions to be understood. The SPARROW model (Preston et al. 2009, 2011) encompasses a hybrid statistical and process-based approach that relates nutrient loads to upstream sources and watershed characteristics using a nonlinear least squares (NLLS) multiple regression. This was used to identify sources and estimate loads of TN and TP to the Sacramento and San Joaquin rivers. SPARROW includes non-conservative

transport, mass-balance constraints, and water flow paths referenced to a digital stream network, National Hydrography Dataset Plus (NHD-Plus) version 2 (<https://nhdplus.com/NHDPlus/>), which defines topography, stream characteristics, and reservoirs as required inputs for the SPARROW model. Potential sources of nutrients to streams throughout the modeled watersheds—such as atmospheric deposition, fertilizer use, geologic sources, wastewater treatment, amounts of land in different use categories, and other potential variables—were based on data for 2012. It is not currently possible to vary these parameters on a yearly basis, so the compromise used in SPARROW is to pick a single reference year, defined as the base year.

SPARROW modeling requires calibration data. The model we used in this summary was part of a greater SPARROW modeling effort, including California, Oregon, and Washington. Data from a total of 307 calibration sites produced the TN and TP models. These sites are located on flow gauging stations and have significant water-quality records to calculate annual loads. Calibration sites need to be in various land-use and climate zones to effectively calibrate the SPARROW model. In addition, all point source dischargers must be known, along with their average annual discharges and all river flow diversions. In addition to water-quality and discharge, land-use data are necessary, and other potential sources of either nitrogen or phosphorus, including atmospheric deposition, geological sources, agricultural sources, and others. Factors which influence transport are also used, such as soil characteristics, slope, rainfall, and groundwater recharge. Sources and transport variables are determined to be either statistically significant or not. Non-significant sources or transport variables are excluded from the model. The calibration procedure and laboratory data used for this SPARROW model are available in Wise (2020).

The SPARROW model includes three types of parameters to predict loads that leave a catchment: sources, land-to-water delivery variables, and instream loss. Water-quality predictors in the model are developed as functions of both

reach and land-surface attributes. They include quantities that describe contaminant sources (point and nonpoint) and factors associated with rates of material transport through the watershed. Details on the theoretical development of the SPARROW model are provided by Alexander et al. (2008) and Schwarz et al. (2006).

RESULTS

Streamflow Trends

Over the 1970-through-2019 period for the Sacramento River at Freeport and the San Joaquin River near Vernalis, there was a decreasing trend in all four annual statistics of daily discharge (7-day minimum daily, median daily, 7-day maximum daily, and mean daily) for both sites (Figures 2 and 3). However, these trends are only statistically significant for annual 7-day minimum daily discharges at the Sacramento River at Freeport with a p -value of 0.033 and a decreasing slope of 0.64% per year (Figure 2). There was no statistically significant trend in all parts of the flow-duration curve over the 365 days of the year for the Sacramento River at Freeport (Figure 4A) for the period of record. On the other hand, at the San Joaquin River near Vernalis, there were some (very likely) negative trends at the medium (50% and 75%) quartile of the flow-duration curve (Figure 4B) (Hirsch et al. 2015). The general lack of trends in stream flow for the period of record can be attributed to flow management by reservoir releases. Reservoir releases can augment low flows during dry years and, similarly, storm flows can be lessened by reservoir storage.

Discharge at the Sacramento River at Freeport and the San Joaquin River near Vernalis vary year to year and are consistent with variable weather conditions during the 1970-through-2019 period. During a high-water year, such as 1997, maximum discharge measurement at the Sacramento River at Freeport and the San Joaquin River near Vernalis reached $3,200 \text{ m}^3 \text{ s}^{-1}$ and $1,537 \text{ m}^3 \text{ s}^{-1}$, respectively. Discharge was much lower in drought years, such as 2012 through 2016, where average measured mean daily discharge at the two sites was about $175 \text{ m}^3 \text{ s}^{-1}$ at Sacramento River

at Freeport and about $9 \text{ m}^3 \text{ s}^{-1}$ at San Joaquin River near Vernalis.

Sacramento River at Freeport, Nutrient Concentrations, Loads, and Trends

Modeled concentrations and loads for the Sacramento River at Freeport are shown in Figure 5. On these and other similar plots, average annual concentrations and annual loads from the model are shown as dots. The flow-normalized concentrations and loads—with confidence intervals calculated for the flow-normalized trends—are shown as a continuous fitted line. Flow-normalized nitrate concentrations and loads follow a similar pattern throughout the 1975-through-2019 period (Figure 5A, 5B). Flow-normalized concentrations and loads of nitrate increase in the earlier period (1975 to 1983), followed by a slight decrease after 1983. Flow-normalized concentrations increased slightly in the late 1980s, and nitrate concentrations and loads reach their highest estimates in 1988 (0.15 mg NL^{-1} and $3.15 \text{ million kg N yr}^{-1}$, respectively). Flow-normalized concentrations declined in the early 1990s and remained stable throughout the mid-1990s and early 2000s and then decreased slightly during the drought period from 2013 through 2015. There is a “likely” increase in flow-normalized concentration (about 0.02 mg NL^{-1}) and loads (about $0.48 \text{ million kg N yr}^{-1}$) over the 1975-through-2019 period (Table 2). A Mann–Whitney–Wilcoxon Rank Sum test was used to compare flow-normalized nitrate concentrations between the early decade (1975 through 1985) and the recent decade (2009 through 2019) on a monthly time-scale (Figure 6A). In the earlier decade, nitrate concentrations were highest in the fall to winter months, compared to the spring and summer.

In contrast, in the recent decade, nitrate concentrations were lower in the winter and increased during the summer, reaching the highest value in June. The median winter (October through March) nitrate concentrations were lower in the recent decade than in the early decade. Conversely, the median summer (May through August) nitrate concentrations were higher in the later decade than the early decade;

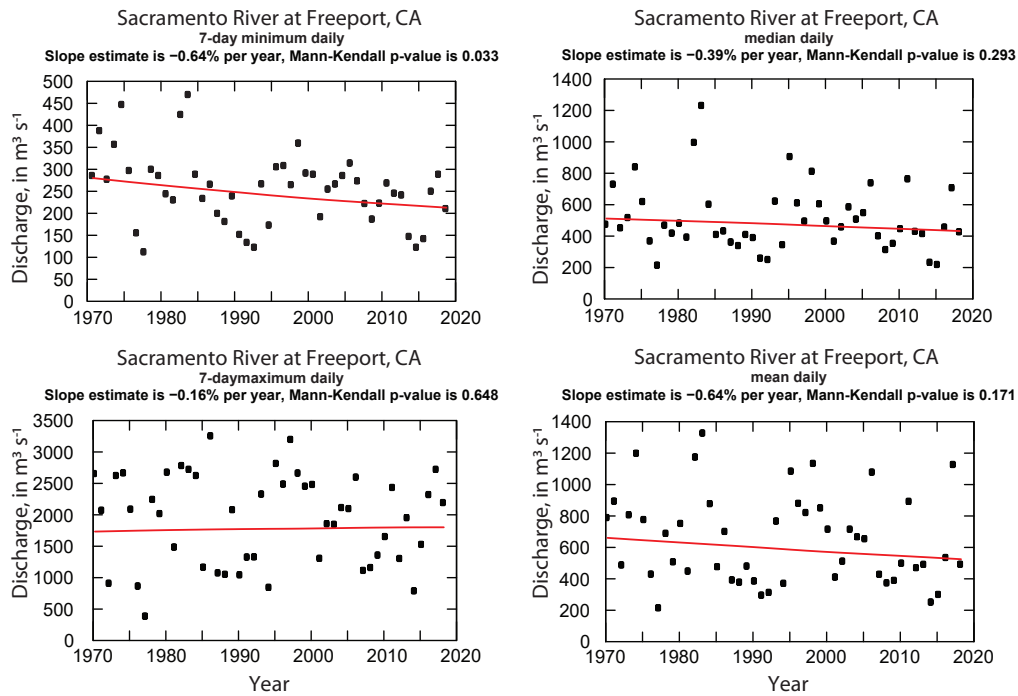


Figure 2 Annual discharge (streamflow) trends for the Sacramento River at Freeport from 1970 to 2019 for four annual discharge statistics: annual minimum day, maximum day, median daily and mean daily. The statistics are determined from the daily discharge record for the stream gauge for the period of record of this study. Each panel shows a Thiel-Sen slope estimate expressed in percentage change per year, and a two-sided p -value for the Mann-Kendall trend test.

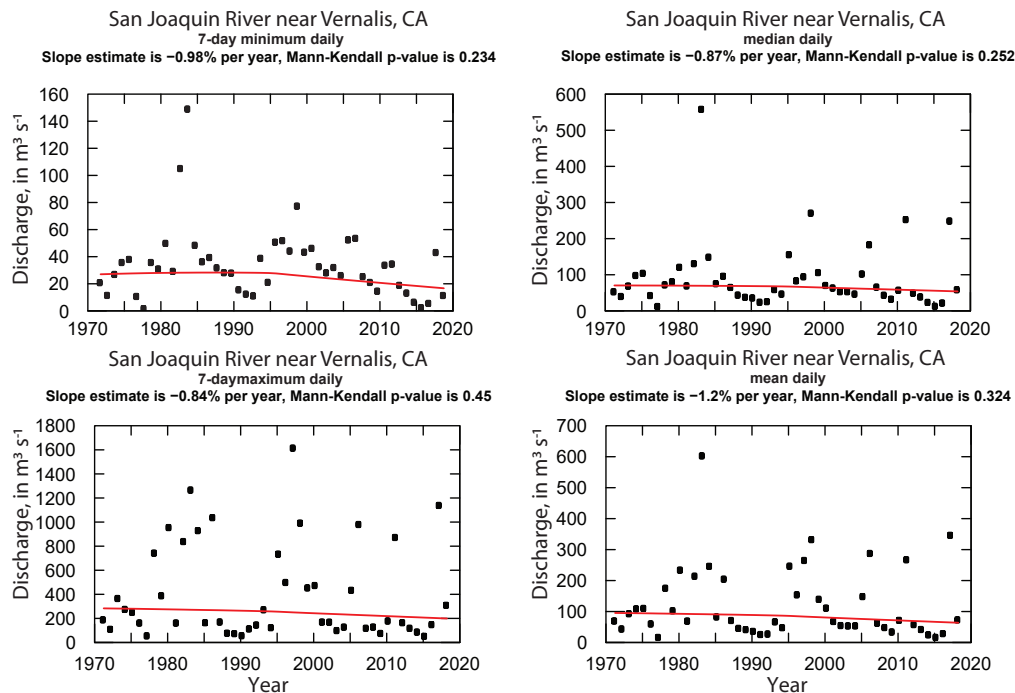


Figure 3 Discharge (streamflow) trends for the San Joaquin River near Vernalis from 1970 to 2019 for four annual discharge statistics: annual minimum day, maximum day, median daily and mean daily. The statistics are determined from the daily discharge record for the stream gauge for the period of record of this study. Each panel shows a Thiel-Sen slope estimate expressed in percentage change per year, and a two-sided p -value for the Mann-Kendall trend test.

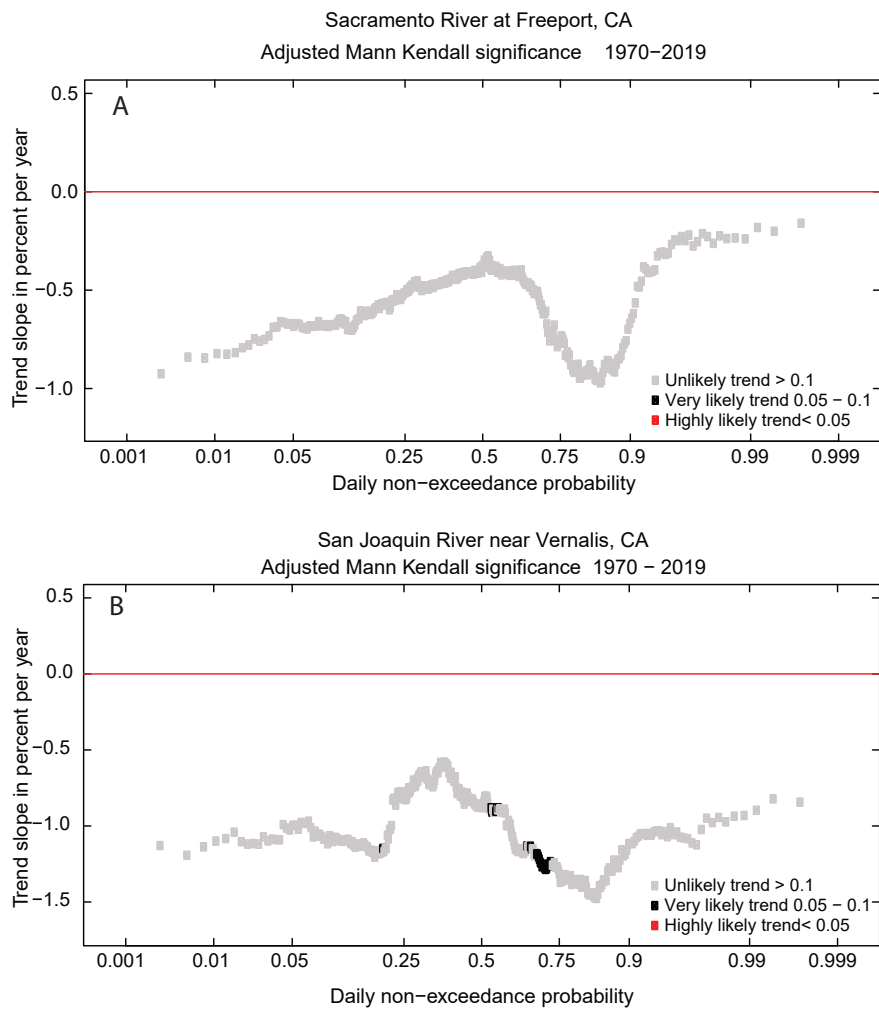


Figure 4 Quantile-Kendall plot showing 1970-through-2019 trends in discharge at (A) Sacramento River at Freeport and (B) San Joaquin River near Vernalis. Daily discharge values were ranked from 1 (the lowest rank) to 365 (the highest rank) within each year. Each *point* represents the estimated trend slope (expressed in percent change per year) for mean daily discharge values of the given rank (1 through 365). Low-flow trends are at the *left* and high-flow trends are at the *right*. Colors indicate, for each rank, the likelihood of the estimated trend slope.

Figure 6C. The median nitrate concentration in April and September did not differ significantly between the early and recent decades, as shown in Figure 6C, where the vertical line crosses the 90% confidence for the median concentration difference between the 2 decades.

Estimated annual concentrations and loads for ammonium (Figure 5) show a different pattern than nitrate. Both concentration and load rapidly declined during the initial modeling period (in 1979, with the highest concentration and load estimated at 0.2 mg N L⁻¹ and 2.7 million kg N yr⁻¹, respectively) followed by a continuous gradual decline in concentration and load to 2019. Variation in estimated flow-normalized ammonium concentrations was low, reflected

in the narrow 90% confidence band (Figures 5C and 5D). Trends in ammonium concentrations and loads at the Sacramento River site were “highly likely” to be decreasing during the 1970-through-2019 period by 0.17 mg N L⁻¹ in concentration and 2.45 million kg N yr⁻¹ in load (Table 2). Figure 6B shows that ammonium concentrations were consistently lower in the recent decade (2009 through 2019) than they were in the early decade (1980 through 1970). This is probably because of the consolidation of wastewater treatment plants that historically discharged into the American River and Sacramento River upstream of Freeport to the SRWTP, which discharges downstream of Freeport. The decrease in median concentrations between the early and recent decades is

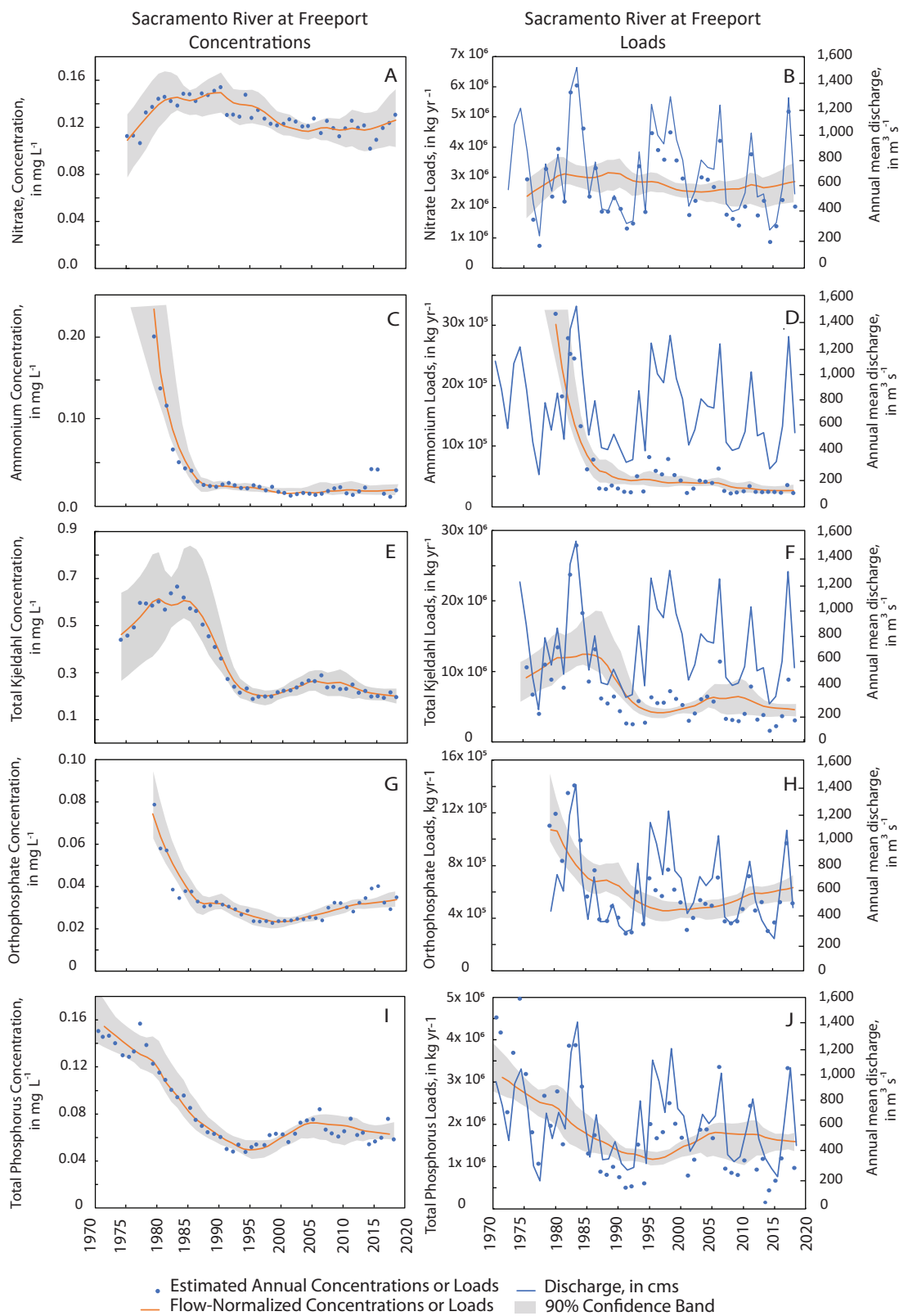


Figure 5 Sacramento River at Freeport models for annual average modeled concentration or load shown in *blue dots* and flow normalized concentration and load in *red lines*. Confidence bands are for flow-normalized concentration or load. *Solid orange line* shows the annual flow-normalized concentration or load. The *blue dots* are the modeled annual mean concentrations and loads. *Solid blue line* is discharge.

Table 2 Trend direction and significance of trends for flow-normalized concentration and load at all sites, and for all constituents for their respective periods of record. [NO₃ CONC nitrate concentration; NH₄ CONC, ammonium concentration; OP CONC, orthophosphate concentration; TKN CONC, total Kjeldahl nitrogen concentration; TP CONC, total phosphorus concentration. *Cell colors* are defined in Table 1.

Site name	NO ₃ CONC, mg N L ⁻¹	NO ₃ Load, kg N yr ⁻¹	NH ₄ CONC mg N L ⁻¹	NH ₄ Load kg N yr ⁻¹	TKN CONC mg N L ⁻¹	TKN Load kg N yr ⁻¹	OP CONC mg P L ⁻¹	OP Load kg P yr ⁻¹	TP CONC mg P L ⁻¹	TP Load kg P yr ⁻¹
Sacramento River at Freeport	Up 0.02	Up 0.48	Down -0.17	Down -2.45	Down -0.26	Down -4.08	Down -0.04	Down -0.57	Down -0.09	Down -1.54
San Joaquin River near Vernalis	Down -0.14	Down -0.27	Down -0.11	Down -0.26	Down -0.78	Down -2.86	Down -0.01	Down -0.05	Down -0.09	Down -0.16

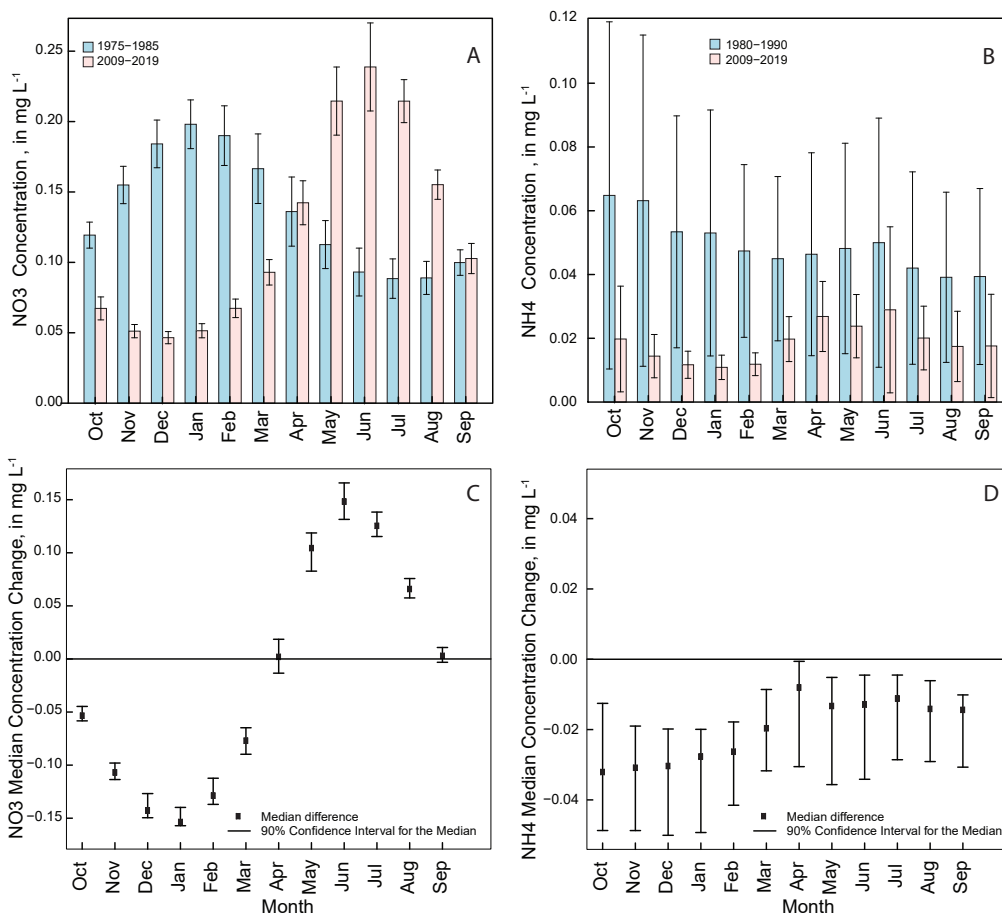


Figure 6 Sacramento River at Freeport monthly side-by-side bar plot showing concentration difference (A, nitrate) and (B, ammonium) between the early (1975-1985) and recent decade (2009-2019). Values are by water year. Monthly median concentration range difference for the early and recent decade and 90% confidence intervals (C and D).

statistically significant for all months of the year (Figure 6D). Annual average ammonium concentrations were higher for 2 drought years near the end of the record (water years 2015 and

2016) because of flow reversal caused by tides near the sampling site at Freeport (Figure 5C). However, this did not affect the flow-normalized trend line.

Trends in Total Kjeldahl nitrogen concentrations and loads follow a similar pattern to that of nitrate (Figures 5E, 5F). Results of the EGRETci test show higher variation in flow-normalized TKN concentrations and loads in the late 1970s and early 1980s, reflected in the wide 90% confidence band during that period. Overall, there is a “very likely” decrease in concentration (about 0.26 mg N L⁻¹) and a “highly likely” decrease in loads (about 4.08 million kg N yr⁻¹) over the 1970-through-2019 period (Table 2).

Orthophosphate concentrations and loads decline in the initial modeling period, down from highs of 0.09 mg P L⁻¹, and 1.1 million kg P yr⁻¹, respectively (Figures 5G and 5H). Flow-normalized concentration or load show little variation within the confidence intervals. Results from the EGRETci test show that there is a “highly likely” decrease in concentration (about 0.04 mg P L⁻¹) and loads (about 0.57 million kg yr⁻¹) over the 1970-through-2019 period (Table 2).

Trends in TP concentration and loads follow a similar pattern (Figures 5I, 5J). After the decline in the TP concentrations and loads in the early part of the record, there is a slight increase to about 0.08 mg P L⁻¹ and 3.1 million kg P yr⁻¹ in 2006, then a gradual decline again through the rest of the period. Overall results from the EGRETci test show that there is a “highly likely” decrease in concentration (about 0.09 mg P L⁻¹) and a “highly likely” decrease in loads (about 1.54 million kg yr⁻¹) over the 1970-through-2019 period (Table 2).

San Joaquin River near Vernalis, Nutrient Concentrations, Loads, and Trends

WRTDS modeling results for the San Joaquin River near Vernalis are shown in Figure 7. Annually averaged flow-normalized nitrate concentrations varied during the 1970-through-2019 period, as did nitrate load (Figure 7A). Results of the EGRETci test indicated a “likely” decrease in concentration (about 0.14 mg N L⁻¹) and loads (about 0.27 million kg N yr⁻¹) over the 1970-through-2019 period (Table 2). Figures 7A and 7B show that the 90% confidence bandwidth for the flow-normalized concentrations and

loads were relatively the same throughout the 1970-through-2019 period. The Mann–Whitney–Wilcoxon Rank Sum test results show that in the early decade nitrate concentrations did not vary much, with the lowest concentrations observed in May and June. Nitrate concentrations were sometimes elevated in the recent decade, particularly in February through April, with the lowest concentrations during July through September (Figure 8A). Median concentration differences between the early and recent decades are only significant in February and July through September (Figure 8C).

Estimated annual concentrations and loads for ammonium show a different pattern than nitrate (Figures 7C, 7D). Ammonium concentrations started to decline around 1980, and continued to decline for the remainder of the period of record (Figure 7C). Variation in estimated loads remains similar throughout the 1970-through-2019 period (Figure 7D). There is a “highly likely” decrease in both concentrations (about 0.11 mg N L⁻¹) and loads (about 0.26 million kg N yr⁻¹) over the 1970-through-2019 period (Table 2). The Mann–Whitney–Wilcoxon Rank Sum test results show that ammonium concentrations decreased in the recent decade (Figure 8B). Unlike nitrate, the difference between the early and recent decade in ammonium concentrations is significant for all months of the year, with high ammonium concentrations in winter for the early decade, and spring for the recent decade (Figures 8B, 8D).

Total Kjeldahl nitrogen concentrations and loads decreased continuously throughout the period of record, like ammonium (Figures 7E, 7F). Results from the EGRETci test also show that there is a “highly likely” decrease in TKN concentrations (about 0.78 mg N L⁻¹) and a “very likely” decrease in loads (about 2.86 million kg N yr⁻¹) over the 1970-through-2019 period (Table 2).

Trends in OP concentrations and loads followed a similar pattern over the 1970-through-2019 period (Figures 7G, 7H). Results from the EGRETci test showed a “likely” decline in both concentrations and loads for the 1970-through-2019 period

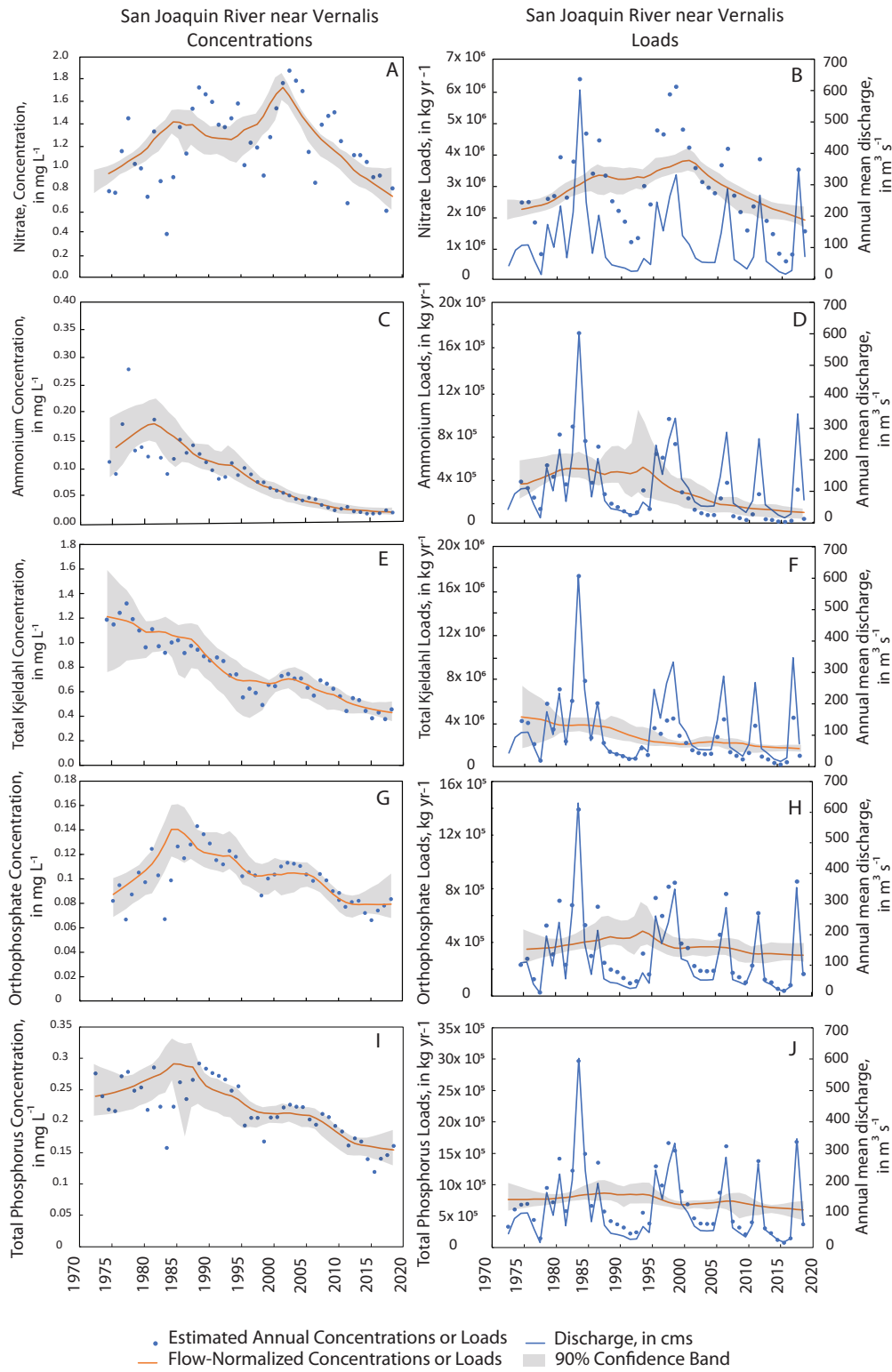


Figure 7 San Joaquin River near Vernalis models for nutrient concentrations and loads. Confidence bands are for flow-normalized concentration or load. Solid orange line shows the annual flow-normalized concentration or load. The blue dots are the modeled annual mean concentrations and loads. Solid blue line is discharge.

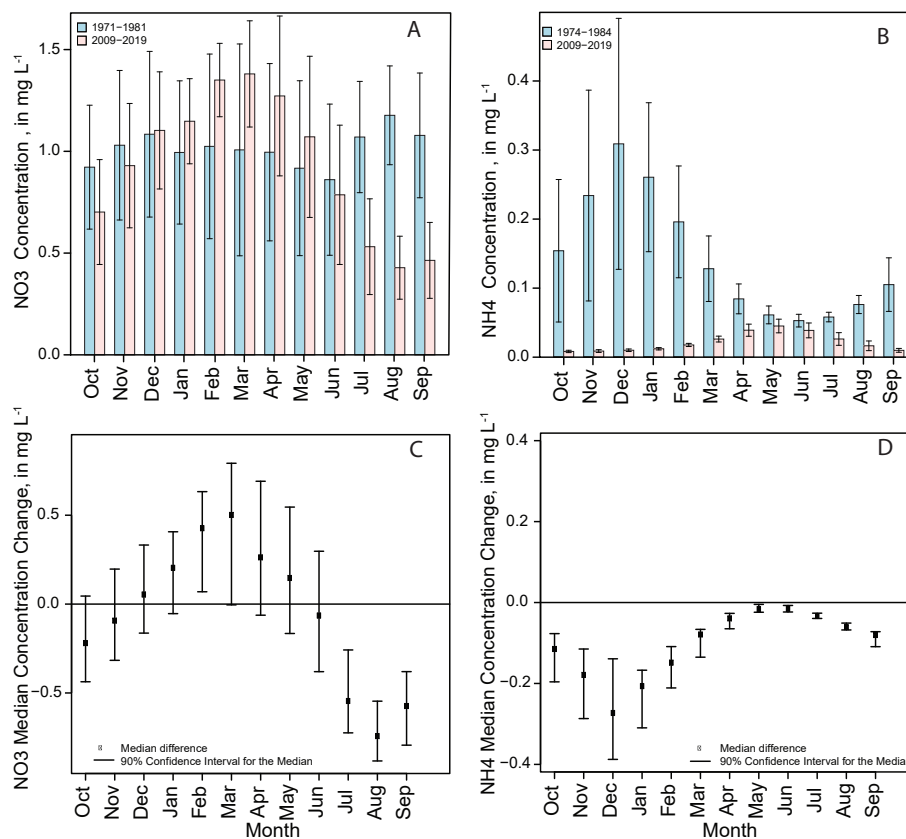


Figure 8 San Joaquin River near Vernalis monthly side-by-side bar plot showing concentration difference (A, nitrate) and (B, ammonium) between the early and recent decade. Monthly median concentration range difference for early and recent decade and 90% confidence intervals (C and D).

(about 0.01 mg PL⁻¹ in concentration and 0.05 million kg Pyr⁻¹ in load).

Trends in TP concentration and loads (Figures 7I, 7J) follow a similar pattern to OP, with a more significant variation in TP concentrations in the mid-80s reflected in the wide 90% confidence band (Figures 7I). Total phosphorus concentrations increased in the early decade to reach their highest value of 0.29 mg PL⁻¹ in 1988, followed by a continued decrease in concentration though the remainder of the period. Overall results from the EGRETCi test show that there are “highly likely” declines in TP concentrations of about 0.09 mg PL⁻¹ and loads of about 0.16 million kg Pyr⁻¹ over the 1970-through-2019 period.

Nutrient Ratios

Modeling of the daily concentrations of the various forms of nitrogen and phosphorus show how dynamic these nutrient ratios are in both the Sacramento and San Joaquin rivers, and how the water chemistry changes with time. Ratios of nitrate to ammonium have changed over the years at both the Sacramento River at Freport and San Joaquin River near Vernalis sites. Time-series plots of modeled daily micromolar concentrations for both locations and ratios of nitrate to ammonium are shown in Figure 9. Both locations show increasing ratios of nitrate to ammonium, and decreasing concentrations of ammonium, for the period of record. Current nitrate-to-ammonium ratios are much higher at the San Joaquin River near Vernalis site because of higher concentrations of nitrate in the water (Figure 9). The median amount of ammonium relative to nitrate at the Sacramento River at

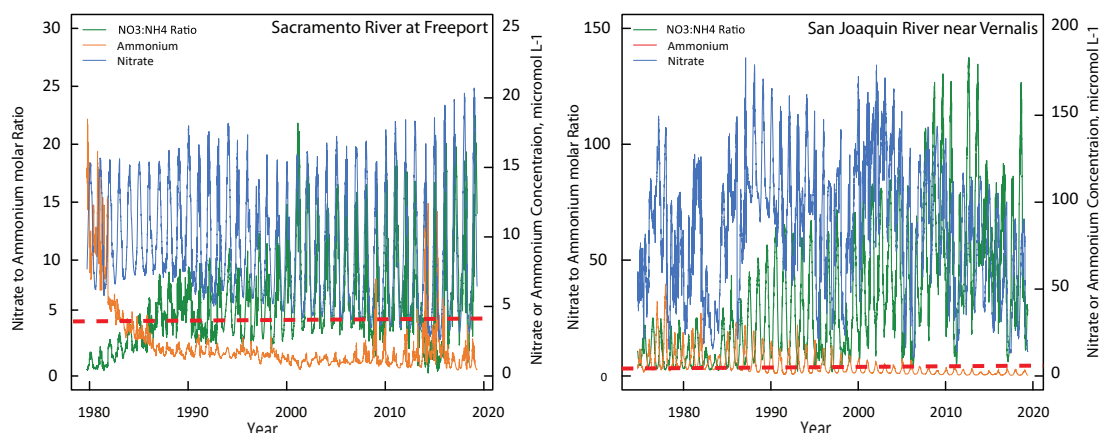


Figure 9 Time-series plots of modeled daily nitrate-to-ammonium ratios and micromolar concentrations of nitrate and ammonium for the Sacramento River at Freeport and San Joaquin River near Vernalis sites. Red dashed line shows concentration of 4 μM ($0.056 \text{ mg N L}^{-1}$) for ammonium.

Freeport site was 19% for the period of record, but current amounts (2019) are between 6% to 7%. In contrast, the current relative amount of ammonium to nitrate (2019) at the San Joaquin River near Vernalis site is between 3% to 4%.

Molar ratios of daily inorganic nitrogen (ammonium plus nitrate) to orthophosphate differ at the Sacramento River and San Joaquin River sites (Figure 10). Nitrate, in particular, is much higher in the San Joaquin River than in the Sacramento River, and there is a much higher ratio of inorganic nitrogen to orthophosphate. How these ratios change throughout an annual cycle is shown with monthly boxplots in Figure 11. The Sacramento River at Freeport site has a molar ratio that is mostly less than the ratio of 24:1 suggested by Maranger et al. (2018), and which drops below 10 during the growing season, indicating a potential for nitrogen-limited water to enter the Delta. In contrast, the San Joaquin River has generally higher molar ratios of nitrogen to phosphorus with more variability, indicating a potential for phosphorus limitation, with ratios that increase during the growing season, possibly due to runoff of nitrate-rich water from the agricultural San Joaquin Valley. Therefore, riverine inputs to the North Delta from the Sacramento River watershed are more likely to indicate nitrogen limitation, whereas riverine inputs to the South Delta are more likely to indicate phosphorus limitation, if nutrient supplies were depleted during periods of rapid

phytoplankton growth (blooms). Although the ratios might indicate limitation for one nutrient over another, there is no indication that current concentrations of either nitrogen or phosphorus are limiting algal productivity.

Nutrient Sources Using SPARROW Model

At the location on the Sacramento River coincident with the Regional San treatment facility discharge, the SPARROW model estimated that about $13.1 \text{ million kg yr}^{-1}$ of TN and $1.5 \text{ million kg yr}^{-1}$ of TP loads are delivered downstream to the Delta. At that location, the annual model estimated that 14.5% of the TN load and 26.9% of the TP loads to the Delta come from treated wastewater effluent discharge to the Sacramento River, some of which originates from upstream locations. Of the 14.5% of the TN load attributed to wastewater, the SPARROW model indicates that half of that—or 7.5%—originates from the Regional San facility and the other 7.5% from other upstream facilities. Of the 26.9% of the wastewater load for TP, 18% of that can be attributed to the Regional San facility, with the remainder originating from upstream wastewater sources. If the Regional San wastewater treatment plant upgrades removed all the nitrogen from the discharge, that would decrease the average annual loading from $13.1 \text{ million kg yr}^{-1}$ of TN to about $11.2 \text{ million kg yr}^{-1}$.

At the San Joaquin River near Vernalis location, the SPARROW model estimated that about

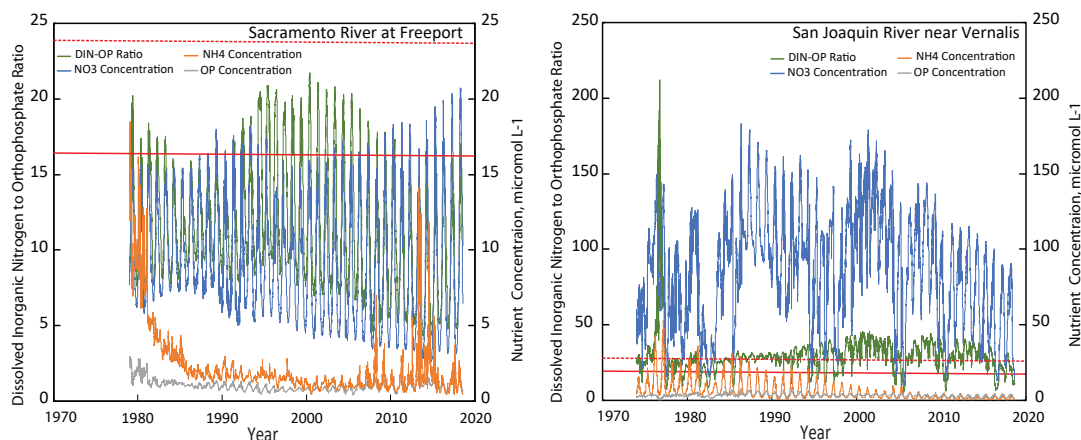


Figure 10 Modeled daily molar ratios of dissolved inorganic nitrogen (nitrate plus ammonium) to inorganic phosphorus (orthophosphate) for the Sacramento River at Freeport and San Joaquin River near Vernalis sites; and nutrient concentrations (nitrate, ammonium, and orthophosphate in micromoles per liter). *Solid red line* indicates Redfield N-to-P ratio (16N:1P). *Dashed red line* indicates proposed N-to-P ratio for freshwater streams (24N:1P).

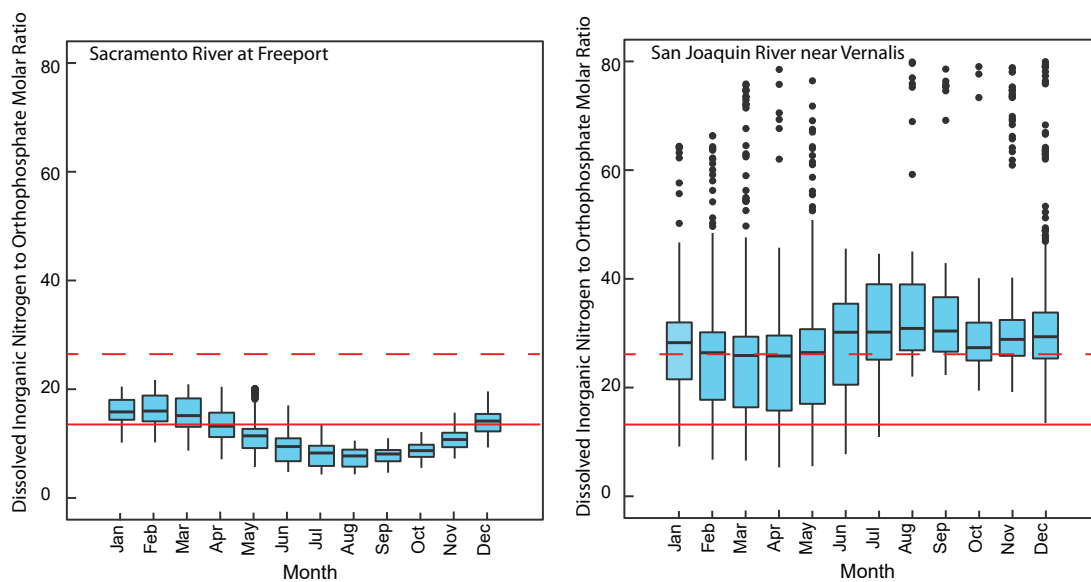


Figure 11 Box and whisker plots of monthly average molar ratios of dissolved inorganic nitrogen (nitrate plus ammonium) to orthophosphate for the Sacramento River at Freeport and San Joaquin River near Vernalis sites for the period of record. Median ratios are shown as the *black line* in each box, *box range* shows the 25th and 75th percentiles box range, and the *whiskers* show the 10th and 90th percentiles. *Solid red line* indicates Redfield N-to-P ratio (16N:1P). *Dashed red line* indicates proposed N-to-P ratio for freshwater streams (24N:1P).

4.8 million kg yr^{-1} of TN and 0.85 million kg yr^{-1} of TP loads are delivered to the Delta. The model estimated about 8.4% of the TN load and 13.3% of the TP loads originates from upstream wastewater facilities such as those near Turlock and Modesto (Figure 1).

Within the Sacramento River watershed, the model identified other major sources of TN as 40% from fertilizer and manure applied to agricultural areas within the Central Valley (Figure 12A, 12B), 31.7% from atmospheric deposition, 8% from scrub and grass land, and 5.8% from urban developed land (Figure 12B). Within the San Joaquin River watershed, the model identified

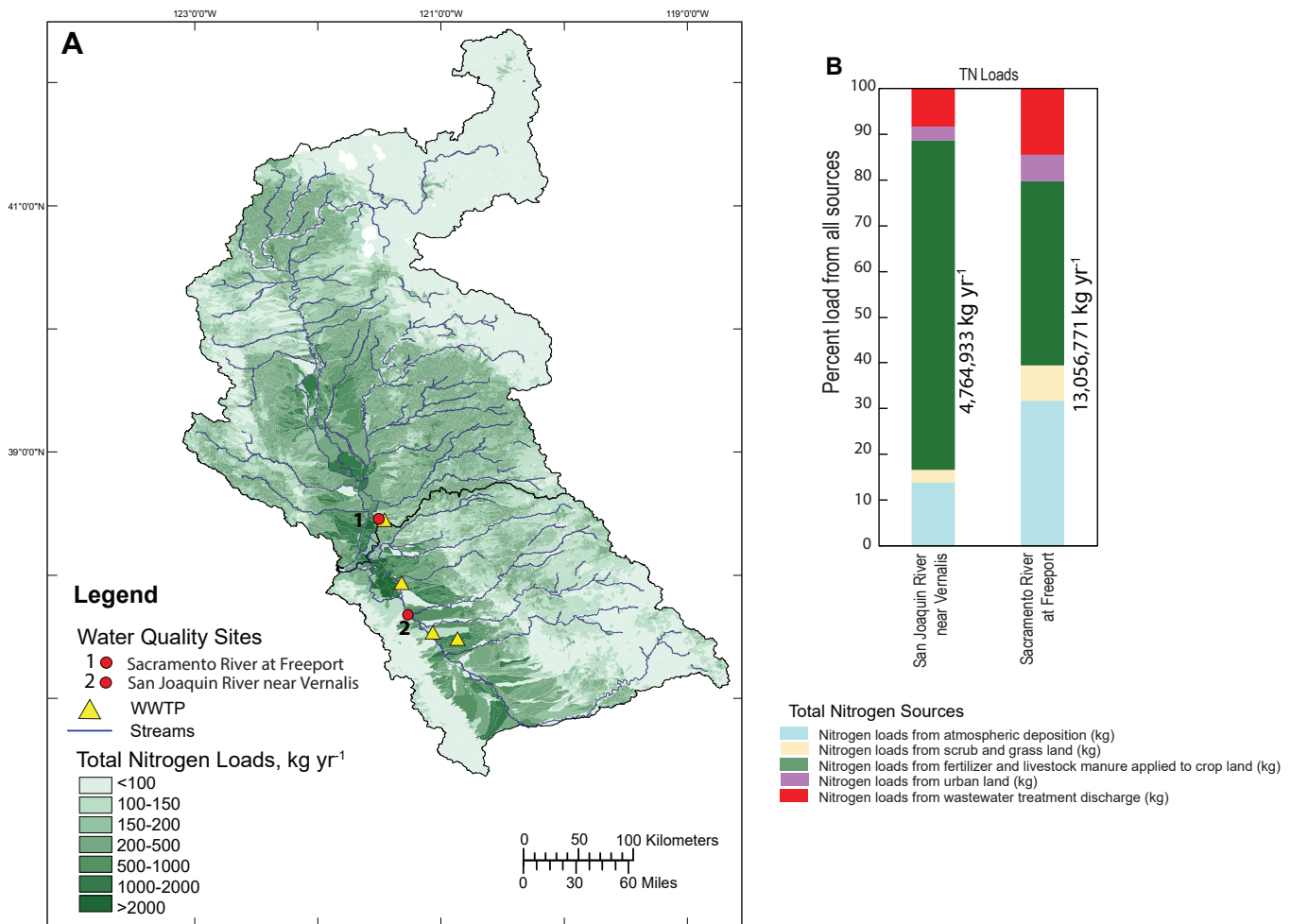


Figure 12 (A) Annual total nitrogen (TN) load exported from the Sacramento and San Joaquin River catchments in kg N yr⁻¹, 2012, as calculated using SPARROW model. (B) Graph shows percent of TN load from all sources in each watershed, as calculated from 2012 SPARROW model.

other major sources of TN as 72.1% from fertilizer and manure, 13.8% from atmospheric deposition, 2.8% from scrub and grass land, and 2.9% from urban runoff (Figure 12B).

Along the 600-km length of the Sacramento River that extends from the headwaters to the Delta, sources of TN vary (Figure 13A). In the headwaters, atmospheric deposition is the main source. As the water moves through the Central Valley, sources change, and loads from fertilizer and livestock manure applications increase at about 150 km from the mouth because of discharges from the Colusa Basin Drain and the Feather River. Downstream of the Sacramento River at Freeport site, TN from point sources

increase because of discharges from the Regional San wastewater treatment plant (Figure 13A). In the headwaters of the San Joaquin River, atmospheric deposition is the main source of TN, and then fertilizer and livestock manure applied to agricultural lands is the major source once the river enters the Central Valley. TN loads from point sources increase at about 150 km from the mouth because of discharge from wastewater treatment facilities in the cities of Turlock and Modesto and increase at about 66 km from the mouth as a result of discharge inputs from the Stockton wastewater treatment facility (Figure 13B).

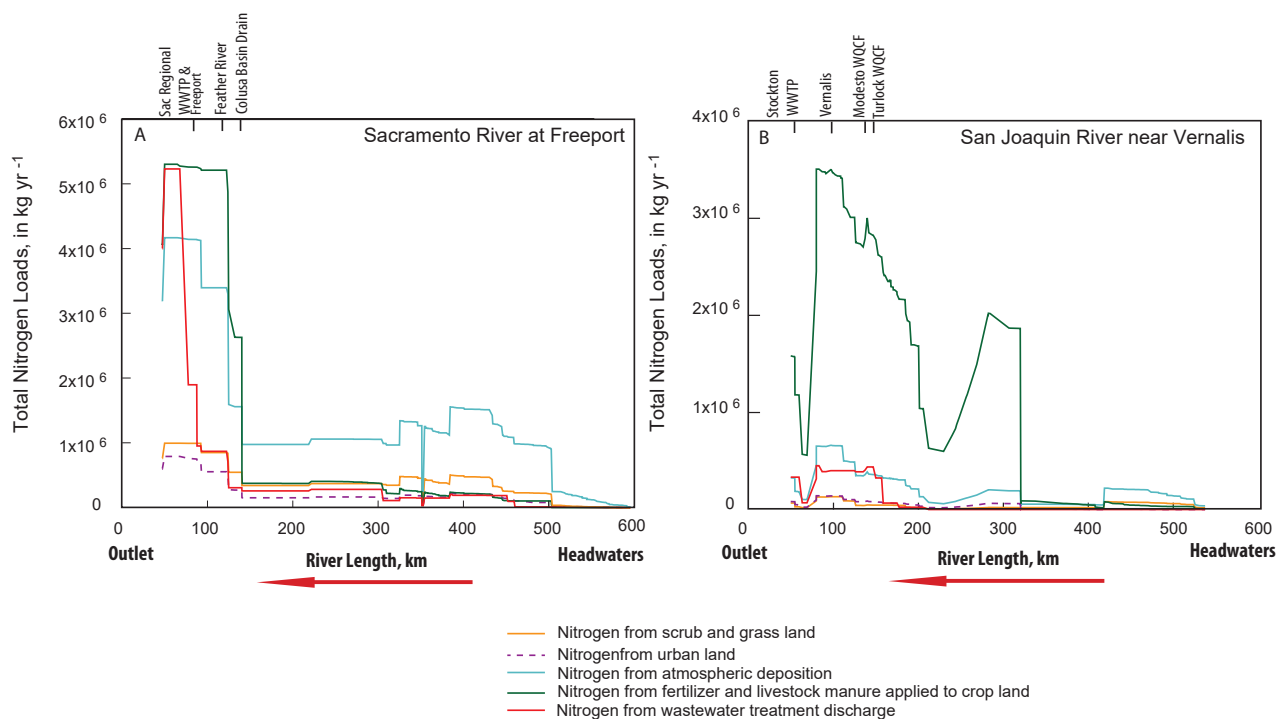


Figure 13 Annual nitrogen loads from various sources in kilograms upstream of the (A) Sacramento River at Freeport and (B) the San Joaquin River near Vernalis from the 2012 SPARROW model

Figure 14A shows the delivered TP loads for each stream reach of the Sacramento and San Joaquin rivers that drain to the Delta. The SPARROW model identified major sources of TP in the Sacramento River watershed as 37.5% from agricultural activities (from fertilizer and manure applications to agricultural lands within the Central Valley), 26.9% from wastewater treatment discharges, 29.9% from geologic phosphorus from the stream channel and upland areas, and 5.7% from urban runoff (Figure 14B). In the San Joaquin River watershed, most TP load (77.2%) originates from fertilizer and manure applications on agricultural land, 13.3% from wastewater treatment facilities, 7.5% from geologic phosphorus from the stream channel and upland areas, and 2% from urban runoff (Figure 14B).

Along the course of the Sacramento River, agricultural activity (from applied fertilizer and manure) accounts for most of the TP loads from the headwaters through the Central Valley until about 70 km from the mouth, when discharges

from the Regional San wastewater treatment plant result in an increase in TP load (Figure 15A). In the San Joaquin River watershed, agricultural activity also accounts for most of the TP load along the river's course. TP loads from point sources increase with the discharges from the Turlock and Modesto wastewater facilities and from the Stockton facility farther downstream (Figure 15B).

DISCUSSION AND CONCLUSIONS

Trend analysis for the Sacramento River at Freeport indicated decreasing ammonium, Kjeldahl nitrogen, orthophosphorus, and total phosphorous concentrations and loads, with a slight increase in nitrate. All modeled nutrients decreased in concentration and load for the San Joaquin River near Vernalis site over the period of record. These results are consistent with a previously published study. Oelsner and Stets (2019), in a study of rivers flowing to coastal regions and the Great Lakes, showed decreasing amounts of total N, including ammonium, and

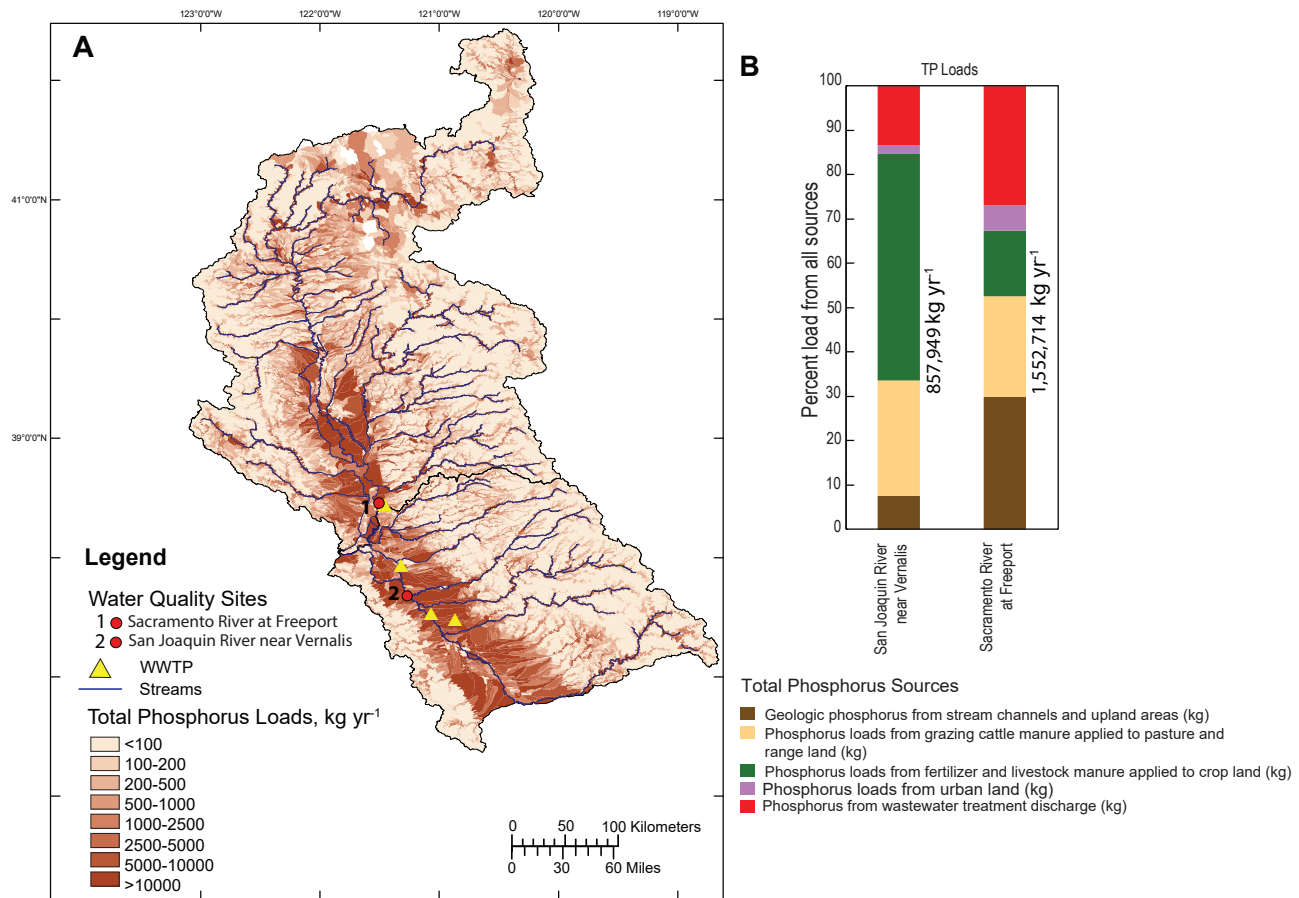


Figure 14 (A) Annual total phosphorus (TP) load exported from the Sacramento and San Joaquin River catchments in kg yr⁻¹, from the 2012 SPARROW model. (B) Graph shows percent of TP load from all sources in each watershed, from the 2012 SPARROW model.

total P for most locations, including rivers of the western US. The Sacramento River at Freeport and the San Joaquin River near Vernalis locations were also included in their analysis. The same technique, WRTDS, was used to model trends for the 2002-through-2012 period. On the other hand, Sprague and Lorenz (2009) modeled trends in TN and TP for 1993 to 2003 using a different technique: the Regional Seasonal Mann-Kendall test. Their study did not observe any significant trends in TN and TP concentrations for sites in the western US during the study period. Comparing results from these two studies shows the power of the WRTDS method, which uses the flow-normalized approach to detect real trends.

SPARROW modeling allows for sources of nutrients to be tracked from upstream portions of the watershed. The SPARROW model used in this study shows loads and sources during an average year by averaging rainfall and de-trending changes in streamflow over a selected period. Therefore, results from the SPARROW model cannot be used to determine changes in loads during years with extreme weather conditions. Nevertheless, the relative amount of TN and TP from various sources provides a good indication of where these loads originate from and identifies changes along the course of either river as land use changes or water is diverted. The catchment for the Sacramento River at Freeport site includes loads that enter the Delta from both areas above Freeport and from the Regional San wastewater

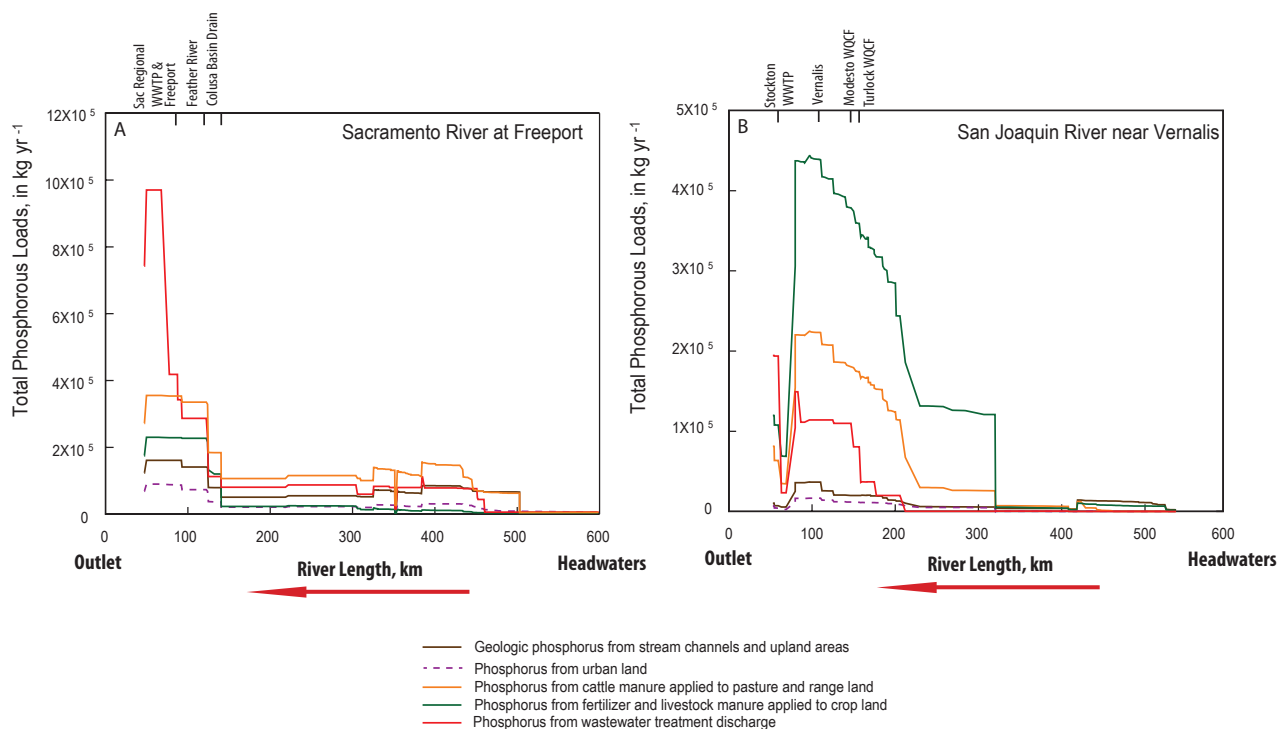


Figure 15 Phosphorus loads from various sources in kilograms upstream of (A) the Sacramento River at Freeport and (B) the San Joaquin River near Vernalis

facility. This source modeling indicates that about 14.5% of the TN that enters the Delta at that portion of the watershed originates from wastewater treatment, both from Regional San and other upstream dischargers. About half of the 14.5% of TN from wastewater dischargers originates upstream of Regional San. The largest source of TN that enters the Delta originates from agricultural operations, the smallest from urban activities. In the Sacramento River watershed, geologic sources and wastewater contribute similar percentages of the TP load to the Delta. In contrast, agricultural operations are dominant sources of TP from the San Joaquin River watershed.

The forms and amounts of individual nutrients can affect aquatic ecology and primary productivity. For example, it has been suggested that ammonium concentrations above $4\ \mu\text{M}$ ($0.056\ \text{mg N L}^{-1}$) can decrease primary productivity (Parker et al. 2012). However, other research has indicated that this may not be the case (Berg et

al. 2017, 2019). Berg et al. (2017, 2019) showed in a field study that although phytoplankton might be stressed in Suisun Bay and other parts of the watershed, that the stressor is not as a result of ammonium, and laboratory studies showed that the growth rate would not be inhibited by the concentrations of ammonium typical in this environment. In the early part of the record, ammonium concentrations exceeded $4\ \mu\text{M}$ at the Sacramento River site until about 1985, and then were consistently less except for drought years such as 2014 and 2015. During drought years, nutrient concentrations were temporarily more than $4\ \mu\text{M}$ because of reverse tidal flows of water in the Sacramento River, which advected nutrients from the Regional San wastewater treatment plant to the sampling location at Freeport. In contrast, ammonium concentrations exceeded $4\ \mu\text{M}$ at the San Joaquin River until about 2004, when the concentrations decreased and remained below that level to the present. Trends in ammonium concentrations and loads decreased at both river sites, especially in the early part of the

study period for the Sacramento River and more gradually at the San Joaquin River. Modeling of these concentrations indicates that both rivers currently have ammonium concentrations below $4\ \mu\text{M}$. Nitrate concentrations in the San Joaquin River are much higher than those in the Sacramento River and, as a result, the nitrate-to-ammonium ratio is much higher.

Ratios of bioavailable nutrients (dissolved inorganic nitrogen to orthophosphate) are dynamic during a year and change with time. Modeled daily molar concentrations of bioavailable dissolved inorganic nitrogen and orthophosphate show changing ratios of bioavailable nitrogen to phosphorus of about 18 to 20 that enter the Delta from the Sacramento River during spring, with declining median ratios in the summer to about 10. This suggests a possible nitrogen-limited system, as phytoplankton pull dissolved nitrate and ammonium out of the water. Although the ratios might suggest a possible nitrogen-limited system, there is no evidence that algal productivity is limited by any one nutrient, or that nutrients are, in fact, limiting algal growth because of their high concentrations in the Bay-Delta system (Cloern and Dufford 2005). In contrast, molar ratios of bioavailable nitrogen to bioavailable phosphorus from the San Joaquin River are elevated throughout the year (Figure 11), with median values of more than 25, which increase to over 30 during the summer. The difference between the two rivers is driven by higher nitrate concentrations in the San Joaquin River from agricultural runoff, compared with the Sacramento River. Therefore, the northern part of the Delta delivers water with lower relative nitrogen in the summer from the Sacramento River, while the southern part of the Delta delivers water with higher nitrogen levels from the San Joaquin River.

Trends in flow-normalized concentrations and loads of most nutrients in the Sacramento River generally show stable conditions around 1990 to 1995, after initial declines. There was a statistically significant increase in nitrate concentration and load for the Sacramento River site in the early part of the record, and all

other nutrients showed statistically significant decreases mainly in the early part of the record and stable conditions after 2000. Unless conditions change regarding land use or climate, these stable flow-normalized conditions may be expected in future years. Although the WRTDS method can successfully predict trends, especially when using flow normalization, actual loads are likely underestimated. A comparative study of the lower Mississippi River (Pellerin et al. 2014), showed that the WRTDS model underestimated nitrate loads compared to loads calculated with a continuous nitrate sensor.

As wastewater sources of dissolved inorganic nitrogen diminish, upstream watershed sources of nitrogen will become the main contributor of loads to the Delta, especially for the North Delta. Agricultural activities in the Central Valley, atmospheric deposition of nitrogen, and runoff from various types of land cover of the Coast Ranges and the Sierra Nevada will be the primary sources of nitrogen to the Delta. Continued monitoring of nutrients that enter the Delta at these two locations is important for land water managers to identify changes in nutrient concentration and loading trends under changing conditions.

ACKNOWLEDGMENTS

This research was funded by the US Geological Survey's Priority Ecosystem Science (PES) Program. We thank Eric Morway for providing R code used for data interpolation, Daniel Wise for his help with the SPARROW 2012 model, as well as Tamara Kraus and Hank Johnson (USGS reviewers), and Timothy Mussen and Lisa Thompson (Regional San reviewers), for their helpful discussion and feedback. Any use of trade, firm, or product names is for descriptive purposes only and does not imply endorsement by the US Government.

REFERENCES

- Alexander R, Smith RA, Schwarz GE, Boyer EW, Nolan JV, Brakebill JW. 2008. Differences in phosphorus and nitrogen delivery to the Gulf of Mexico from the Mississippi River Basin. *Environ Sci Technol*. [accessed 2021 Oct 1];42(3):822–830. <https://doi.org/10.1021/es0716103>
- Beck MW, Jabusch TW, Trowbridge PR, Senn DB. 2018. Four decades of water quality change in the upper San Francisco Estuary. *Estuar Coast Shelf Sci*. [accessed 2021 Oct 1];212:11–22. <https://doi.org/10.1016/j.ecss.2018.06.021>
- Berg GM, Driscoll S, Hayashi K, Kudela R. 2019. Effects of nitrogen source, concentration, and irradiance on growth rates of two diatoms endemic to northern San Francisco Bay. *Aquat Biol*. [accessed 2021 Oct 1];28:33–43. <https://doi.org/10.3354/ab00708>
- Berg GM, Hayashi K, Ross M, Kudela R. 2017. Variation in growth rate, carbon assimilation, and photosynthetic efficiency in response to nitrogen source and concentration in phytoplankton isolated from upper San Francisco Bay. *J Phycol*. [accessed 2021 Oct 1];53:664–679. <https://doi.org/10.1111/jpy.12535>
- Bureau J, Ruhl C, Work P. 2015. Innovation in monitoring: the US Geological Survey Sacramento–San Joaquin River Delta, California, flow-station network. *US Geological Survey Fact Sheet 2015–3061*. [accessed 2021 Oct 1]. 6 p. <https://doi.org/10.3133/fs20153061>
- Cloern JE, Dufford R. 2005. Phytoplankton community ecology: principles applied in San Francisco Bay. *Mar Ecol Prog Ser* [accessed 2021 Oct 1];285:11–28. <https://doi.org/10.3354/meps285011>
- Domagalski JL, Morway E, Alvarez NL, Hutchins J, Rosen MR, Coats R. 2021. Trends in nitrogen, phosphorus, and sediment concentrations and loads in streams draining to Lake Tahoe, California, Nevada, USA. *Sci Total Environ*. [accessed 2021 Oct 1];752:141815. <https://doi.org/10.1016/j.scitotenv.2020.141815>
- Domagalski J, Saleh D. 2015. Sources and transport of phosphorus to rivers in California and adjacent states, US, as determined by SPARROW Modeling. *J Am Water Resour Assoc*. [accessed 2021 Oct 1];51:1463–1486. <https://doi.org/10.1111/1752-1688.12326>
- Fishman MJ. 1993. Methods of analysis by the US Geological Survey National Water Quality Laboratory-determination of inorganic and organic constituents in water and fluvial sediments. Reston (VA): USGS. Open-File Report 93-125. [accessed 2021 Oct 1]. Available from: <https://doi.org/10.3133/ofr93125>
- Fox P, Hutton PH, Howes DJ, Draper AJ, Sears L. 2015. Reconstructing the natural hydrology of the San Francisco Bay–Delta watershed. *Hydrol Earth Syst Sci*. [accessed 2021 Oct 1];19:4257–4274. <https://doi.org/10.5194/hess-19-4257-2015>
- Glibert PM. 2010. Long-term changes in nutrient loading and stoichiometry and their relationships with changes in the food web and dominant pelagic fish species in the San Francisco Estuary. California. *Rev Fish Sci*. [accessed 2021 Oct 1];18(2):211–232. <https://doi.org/10.1080/10641262.2010.492059>
- Hirsch RM, Archfield SA, De Cicco LD. 2015. A bootstrap method for estimating uncertainty of water quality trends. *Environ Model Softw*. [accessed 2021 Oct 1];73:148–166. <https://doi.org/10.1016/j.envsoft.2015.07.017>
- Hirsch RM, Moyer DL, Archfield SA. 2010. Weighted regressions on time, discharge, and season (WRTDS), with an application to Chesapeake Bay river inputs. *J Am Water Resour Assoc*. [accessed 2021 Oct 1];46:857–880. <https://doi.org/10.1111/j.1752-1688.2010.00482.x>
- Jassby AD, Cloern JE. 2000. Organic matter sources and rehabilitation of the Sacramento–San Joaquin Delta (California, USA). *Aquat Conserv*. [accessed 2021 Oct 1];10:323–352. <https://onlinelibrary.wiley.com/doi/10.1002/1099-0755%28200009/10%2910%3A5%3C323%3A%3AAID-AQC417%3E3.0.CO%3B2-J>
- Kratzer CR, Kent RH, Saleh DK, Knifong DL, Dileanis PD, Orlando JL. 2011. Trends in nutrient concentrations, loads, and yields in streams in the Sacramento, San Joaquin, and Santa Ana basins, California, 1975–2004. *US Geological Survey Scientific Investigations Report 2010-5228*. [accessed 2021 Oct 1]. 112 p. <https://pubs.usgs.gov/sir/2010/5228>

- Krich–Brinton A. 2017. Projected nutrient load reductions to the Sacramento–San Joaquin Delta associated with changes at four POTWs. Memorandum dated January 25, 2017, to Terrie Mitchell, SRCSD, from Larry Walker Associates. [accessed 2021 Oct 1]. Available from: https://www.waterboards.ca.gov/rwqcb5/water_issues/delta_water_quality/delta_nutrient_research_plan/science_work_groups/2017_0417_massbal_memo.pdf
- Luoma SN, Dahm CN, Healy M, Moore JN. 2015. Challenges facing the Sacramento–San Joaquin Delta: complex, chaotic, or simply cantankerous? *San Franc Estuary Watershed Sci.* [accessed 2021 Oct 1];13:3. <https://doi.org/10.15447/sfews.2015v13iss3art7>
- Maavara T, Akbarzadeh Z, Van Cappellen P. 2020. Global dam-driven changes to riverine N:P:Si ratios delivered to the coastal ocean. *Geophys Res Lett.* [accessed 2021 Oct 1];47:e2020GL088288. <https://agupubs.onlinelibrary.wiley.com/doi/10.1029/2020GL088288>
- Maranger R, Jones, SE, Cotner, JB. 2018. Stoichiometry of carbon, nitrogen, and phosphorus through the freshwater pipe. *Limnol Oceanogr Lett.* [accessed 2021 Oct 1];3:89–101. <https://aslopubs.onlinelibrary.wiley.com/doi/10.1002/lol2.10080>
- Norgaard RB, Kallis G, Kiparsky M. 2009. Collectively engaging complex socio-ecological systems: re-envisioning science, governance, and the California Delta. *Environ Sci Policy.* [accessed 2021 Oct 1];12:644–652. <https://doi.org/10.1016/j.envsci.2008.10.004>
- Oelsner GP, Stets EG. 2019. Recent trends in nutrient and sediment loading to coastal areas of the conterminous US: insights and global context. *Sci Total Environ.* [accessed 2021 Oct 1];654:1225–1240. <https://doi.org/10.1016/j.scitotenv.2018.10.437>
- Parker AE, Dugdale RC, Wilkerson FP. 2012. Elevated ammonium concentrations from wastewater discharge depress primary productivity in the Sacramento River and the northern San Francisco Estuary. *Mar Pollut Bull.* [accessed 2021 Oct 1];64:574–586. <https://doi.org/10.1016/j.marpolbul.2011.12.016>
- Pellerin BA, Bergamaschi BA, Gilliom RJ, Crawford CG, Saraceno J, Frederick CP, Downing BD, Murphy JC. 2014. Mississippi River nitrate loads from high frequency sensor measurements and regression-based load estimation. *Environ Sci Technol.* [accessed 2021 Oct 1];48:12612–12619. <https://doi.org/10.1021/es504029c>
- Preston SD, Alexander RB, Wolock DM. 2011. Sparrow modeling to understand water-quality conditions in major regions of the United States: a featured collection introduction. *J Am Water Resour Assoc* [accessed 2021 Oct 1];47(5):887–890. <https://doi.org/10.1111/j.1752-1688.2011.00585.x>
- Preston SD, Alexander RB, Woodside MD, Hamilton PA. 2009. SPARROW MODELING—enhancing understanding of the nation’s water quality. [accessed 2021 Oct 1]. US Geological Survey Fact Sheet 2009-3019. 6 p. Available from: <http://pubs.usgs.gov/fs/2009/3019>
- Redfield AC. 1958. The biological control of chemical factors in the environment. *Am Sci.* [accessed 2021 Oct 1];46:205–221. <https://www.jstor.org/stable/27827150>
- Richey A, Robinson A, Senn D. 2018. Operation baseline science and monitoring needs: a memorandum summarizing the outcomes of a stakeholder workshop and surveys. [accessed 2021 Oct 1]. Available from: https://sfbaynutrients.sfei.org/sites/default/files/final_regional_san_workshop_memo_10.03.2018.pdf
- Saleh D, Domagalski J. 2015. SPARROW modeling of nitrogen sources and transport in rivers and streams of California and adjacent states, U.S. *J Am Water Resour Assoc.* [accessed 2021 Oct 1];51:1487–1507. <https://doi.org/10.1111/1752-1688.12325>
- Sauer VB, Turnipseed DP. 2010. Stage measurement at gaging stations. Chapter A7 In: *US Geological Survey techniques and methods, book 3.* [accessed 2021 Oct 1]. 45 p. Available from: <https://pubs.er.usgs.gov/publication/tm3A7>
- Schlegel B, Domagalski JL. 2015. Riverine nutrient trends in the Sacramento and San Joaquin basins, California: a comparison to state and regional water quality policies. *San Franc Estuary Watershed Sci.* [accessed 2021 Oct 1];13(4). <https://doi.org/10.15447/sfews.2015v13iss4art2>

- Schwarz GE, Hoos AB, Alexander RB, Smith RA. 2006. Section 3: the SPARROW surface water-quality model—theory, application, and user documentation. [accessed 2021 Oct 1]. US Geological Survey techniques and methods, 6-B3. 248 p. <https://doi.org/10.3133/tm6B3>
- Sprague LA, Lorenz DL. 2009. Regional nutrient trends in streams and rivers of the United States, 1993–2003. *Env Sci Technol*. [accessed 2021 Oct 1];43(10):3430–3435. <https://doi.org/10.1021/es803664x>
- Templin WE, Cherry DE. 1997. Drainage-return, surface-water withdrawal, and land-use data for the Sacramento–San Joaquin Delta, with emphasis on Twitchell Island, California. Sacramento (CA): US Geological Survey. Open-File Report 97-350. [accessed 2021 Oct 1]. 31 p. Available from: <https://pubs.er.usgs.gov/publication/ofr97350>
- Turnipseed DP, Sauer VB. 2010. Discharge measurements at gaging stations. Chapter A8. In: US Geological Survey techniques and methods, book 3. p. 87. [accessed 2021 Oct 1]. Reston (VA): US Geological Survey. <https://pubs.er.usgs.gov/publication/tm3A8>
- [USGS] US Geological Survey. 2020. National Water Information System [NWIS]: USGS web interface. [accessed 2021 Oct 1]. <https://doi.org/10.5066/F7P55KJN>
- Wise DR. 2020. Spatially referenced models of streamflow and nitrogen, phosphorus, and suspended-sediment loads in streams of the Pacific region of the United States. (Version 1.1). [accessed 2021 Oct 1]. US Geological Survey Scientific Investigations Report 2019-5112. 64 p. <https://doi.org/10.3133/sir20195112>
- West Yost Associates. 2011. Wastewater control measures study. Prepared for Central Valley Regional Water Quality Control Board Drinking Water Policy Workgroup. Report 304-06-10-06. [accessed 2021 Oct 1]. 64 p. Available from: http://www.waterboards.ca.gov/centralvalley/water_issues/drinking_water_policy/dwp_wastewtr_cntrl_meas_stdy.pdf